ISSN No:-2456-2165 https://doi.org/10.38124/ijisrt/26jun1770

Comparative Validation of Groundwater Potential Zone Models Using VES, Borehole Records, and GIS/Remote Sensing in the Precambrian Basement of FCT Abuja: An AUC–ROC Performance Assessment

Ado Umar Farouq[1]

[1]Industrial Safety & Environmental Technology Department, Petroleum Training Institute Effurun, Delta State, Nigeria

Publication Date: 2026/07/22

Abstract: Groundwater remains the principal source of potable water supply in the Federal Capital Territory (FCT), Abuja, Nigeria, where rapid urbanization and increasing water demand have intensified pressure on the fractured Precambrian Basement Complex aquifer system. Reliable groundwater potential zone (GPZ) mapping is therefore essential for sustainable groundwater exploration and management. This study comparatively evaluated and validated groundwater potential models developed from Geographic Information Systems and Remote Sensing (GIS/RS), Vertical Electrical Sounding (VES), and borehole productivity records using the Analytical Hierarchy Process (AHP). Eight groundwater-conditioning factors; rainfall, geology, slope, drainage density, lineament density, land use/land cover, soil type, and Topographic Wetness Index (TWI) were integrated within a GIS environment to develop the GIS/RS model, while aquifer thickness, overburden thickness, aquifer resistivity, and depth to aquifer were used for the VES model, and discharge, drawdown, and recovery parameters constituted the borehole model. The AHP assigned the highest weights to rainfall (33.1%), geology (23.3%), and slope (14.2%), with an acceptable consistency ratio (CR = 0.0456), confirming the reliability of the weighting scheme. The GIS/RS, VES, and borehole models delineated 612.56 km² (8.56%), 75.45 km² (1.00%), and 366.22 km² (4.84%) as high groundwater potential zones, respectively. Integration of the three datasets produced a refined groundwater potential map comprising 708.85 km² (9.40%) of high, 6,746.69 km² (89.46%) of moderate, and 85.71 km² (1.14%) of low groundwater potential. Model validation using Receiver Operating Characteristic (ROC) analysis demonstrated good to very good predictive performance. The GIS/RS model achieved an AUC of 0.820 (AOC = 0.180) with 85.6% sensitivity, while the VES model recorded an AUC of 0.790 (AOC = 0.210) and 93.3% sensitivity. The borehole model exhibited the highest standalone predictive accuracy (AUC = 0.860, AOC = 0.140, sensitivity = 94.2%), whereas the integrated model achieved an AUC of 0.845 (AOC = 0.155) with 93.8% sensitivity, providing the best balance between predictive accuracy and spatial representation. The study demonstrates that integrating GIS/RS, VES, and borehole datasets substantially enhances the reliability of groundwater potential mapping and provides a robust scientific framework for groundwater exploration, borehole siting, and sustainable water resource management in the FCT and other Precambrian Basement Complex terrains.

Keywords: *Groundwater Potential Zone, AHP, GIS, Remote Sensing, ROC Curve, AUC, Vertical Electrical Sounding, Borehole Yield, Basement Complex, Abuja.*

How to Cite: Ado Umar Farouq (2026) Comparative Validation of Groundwater Potential Zone Models Using VES, Borehole Records, and GIS/Remote Sensing in the Precambrian Basement of FCT Abuja: An AUC–ROC Performance Assessment. *International Journal of Innovative Science and Research Technology,* 11(6), 3855-3874. https://doi.org/10.38124/ijisrt/26jun1770

I. INTRODUCTION

Groundwater constitutes one of the most important freshwater resources globally and serves as a critical component of water supply systems, particularly in semi-arid and developing regions. In Nigeria, groundwater supplies a substantial proportion of domestic, agricultural, and industrial water demands. Within the Federal Capital Territory (FCT), Abuja, rapid population growth, urban expansion, and climate variability have intensified dependence on groundwater resources.

ISSN No:-2456-2165 https://doi.org/10.38124/ijisrt/26jun1770

However, increasing groundwater abstraction, coupled with unregulated borehole drilling, has contributed to a significant decline in groundwater levels, as reflected by the increase in average borehole depths from approximately 40 m to 80 m over the past decade (Ibrahim *et al.,* 2024). In addition, inadequate hydrogeological and geophysical site investigations prior to borehole construction have resulted in frequent borehole failures and persistent water scarcity; Borehole failure rates approaching 36% within the FCT further highlight the necessity for systematic pre-drilling geophysical assessments to optimize groundwater development and minimize economic losses (Alao *et al.*, 2024b).

This study employs advanced electrical resistivity techniques to delineate fractured basement aquifers, which constitute the principal groundwater reservoirs within crystalline basement terrains (Osumeje *et al.,* 2023). Through the integration of Vertical Electrical Sounding (VES) data and borehole lithological information, the research provides a comprehensive evaluation of subsurface stratigraphy aimed at improving groundwater exploration success rates. The study focuses on characterizing the geoelectric signatures of the Basement Complex terrain, where groundwater occurrence is predominantly controlled by secondary porosity associated with fractured crystalline rocks (Farouq *et al.,* 2025). Consequently, geophysical methods provide an effective means of identifying high-transmissivity zones that may not be detectable through conventional drilling approaches. Furthermore, these techniques are advantageous because of their non-invasive nature, cost-effectiveness, and capacity to provide rapid and reliable interpretations of subsurface conditions compared with many alternative exploration methods (Adeniji *et al.,* 2013).

The application of electrical resistivity methods is particularly important in Basement Complex terrains, where groundwater storage depends largely on the development of fractures, joints, and weathered overburden materials (Omeje *et al.,* 2015a; Omeje *et al.,* 2015b). Electrical resistivity surveys facilitate the identification of these weathered and fractured zones by measuring variations in subsurface resistivity resulting from changes in lithology, porosity, and water saturation (Emmanuel *et al.,* 2024; Jimoh *et al.,* 2023). Mapping such resistivity contrasts enables the delineation of aquiferous units that are critical for sustainable groundwater development in basement environments characterized by generally low aquifer yields (Abdulbariu *et al.,* 2024). Consequently, accurate characterization of aquifer geometry and hydrogeological properties remains essential for ensuring the long-term sustainability of groundwater abstraction systems.

The hydrogeology of the FCT is predominantly controlled by Precambrian Basement Complex rocks comprising granites, migmatites, schists, gneisses, and quartzites. Groundwater occurrence within these crystalline formations is generally restricted to weathered regolith and fractured bedrock zones. As a result, successful groundwater exploration requires the accurate delineation of these heterogeneous subsurface units because aquifer productivity is strongly influenced by secondary porosity generated through tectonic fracturing (Mangs *et al.,* 2023). Groundwater storage and movement within the crystalline basement depend on the degree of weathering and the extent of interconnected fracture systems (Naiyeju *et al.,* 2021). The occurrence of NNE–SSW trending fractures and joints has been identified as an important structural indicator for locating productive groundwater zones because of their tendency to form interconnected flow pathways within the basement rocks (Sunkari *et al.,* 2021). These structural features enhance hydraulic conductivity and facilitate the development of localized high-yield aquifers within otherwise low-permeability bedrock formations (Olorunfemi *et al.,* 2020). Accordingly, geophysical methods, particularly electrical resistivity imaging, play a vital role in identifying and characterizing these groundwater-bearing zones (Ogundana & Falae, 2024).

Recent developments in Geographic Information Systems (GIS), Remote Sensing (RS), Multi-Criteria Decision Analysis (MCDA), and geophysical exploration techniques have substantially enhanced groundwater potential mapping. Among these approaches, the Analytical Hierarchy Process (AHP) has gained widespread acceptance because it enables the systematic weighting of groundwater conditioning factors based on expert knowledge while effectively handling complex geospatial datasets (Baghel *et al.*, 2023; Jhariya *et al.*, 2016). Through hierarchical pairwise comparisons, AHP reduces subjectivity in determining the relative importance of hydrogeological variables (Ajayi *et al.*, 2022; Rajesh *et al.,* 2021).

Furthermore, the integration of thematic layers within GIS environments facilitates the delineation of groundwater potential zones and provides a robust framework for sustainable groundwater management (Ajadi *et al.,* 2025; Zewdie *et al.,* 2024). Such integrated approaches are particularly useful in remote or topographically complex regions where conventional field investigations are difficult and costly (Arulbalaji *et al.,* 2019; Shekar & Mathew, 2023). Moreover, the combination of high-resolution satellite imagery and MCDA techniques supports informed decision-making for water resource planning and land-use management (Pandian *et al.,* 2023; Taher *et al.,* 2023).

Despite the extensive application of GIS-based groundwater potential mapping, model validation remains a major challenge. Many groundwater potential maps are produced without independent verification using field-based hydrogeological or geophysical datasets, a limitation reported in approximately 15% of recent groundwater studies (Bennett, 2023). Consequently, the absence of reliable ground-truth information, such as borehole yield records and long-term groundwater monitoring data, often reduces the credibility and predictive reliability of groundwater potential models (Gandhi *et al.,* 2024; Musekiwa *et al.,* 2025).

Additionally, subjectivity in assigning weights to thematic layers, combined with limitations in the availability of high-resolution geomorphological and soil datasets, introduces further uncertainty into model outputs (Abera &

ISSN No:-2456-2165 https://doi.org/10.38124/ijisrt/26jun1770

Gebre-Egziabher, 2024). To address these limitations, recent studies have increasingly adopted Receiver Operating Characteristic (ROC) analysis and step-drawdown testing as quantitative validation tools for assessing model performance against observed groundwater data (Bayode *et al.*, 2024). ROC analysis generates Area Under the Curve (AUC) values that provide a robust measure of model predictive accuracy and discrimination capability (Pande *et al.*, 2021; Shinde *et al.*, 2024). Generally, AUC values greater than 0.80 indicate strong predictive performance and high model reliability (Dars *et al.*, 2024; Roy *et al.*, 2024). The validation process typically involves comparing model outputs with observed borehole yields and known groundwater occurrences to evaluate model effectiveness under real hydrogeological conditions (Jothibasu & Anbazhagan, 2016; Salem *et al.*, 2025).

This study therefore aims to comparatively evaluate and validate groundwater potential zone models developed from GIS/Remote Sensing, Vertical Electrical Sounding (VES), and borehole productivity records using Receiver Operating Characteristic (ROC) analysis and Area Under the Curve (AUC) performance assessment.

The study aimed to delineate groundwater potential zones using Geographic Information Systems (GIS), Remote Sensing (RS), and the Analytical Hierarchy Process (AHP); characterize aquifer conditions through geoelectrical parameters derived from Vertical Electrical Sounding (VES) data; develop groundwater potential models based on borehole productivity records; validate and compare the predictive performance of GIS-, VES-, and borehole-based models using Receiver Operating Characteristic–Area Under the Curve (ROC–AUC) analysis; and ultimately identify the most reliable approach for groundwater exploration within the Precambrian Basement Complex terrain of the Federal Capital Territory (FCT), Abuja.

➢ *Study Area*

The Federal Capital Territory is characterized by a Guinea Savannah vegetation zone dominated by grasses and scattered woodland species (Ebukiba & Adamu, 2020; Sanusi *et al.*, 2021). Toward the southern parts of the territory, the vegetation gradually transitions into denser tropical rainforest formations, whereas the northern sections exhibit relatively drier savannah conditions (Obiadi *et al.*, 2019). These diverse ecological settings support an extensive drainage network that contributes to the Niger and Benue River systems (Ideki & Weli, 2019). Major rivers, including the Gwagwalada and Usmanu Rivers, display predominantly dendritic to trellis drainage patterns and depend largely on seasonal rainfall for hydrological recharge (Akoachere *et al.*, 2019).

Geomorphologically, the region is characterized by undulating plains interspersed with inselbergs and mountainous terrains that influence local climatic conditions and rainfall distribution through orographic effects (Awuh *et al.*, 2019). Prominent geological landmarks such as Zuma Rock and Aso Rock serve as significant topographic features that influence hydrological boundaries and patterns of urban development within the territory (NOMA *et al.*, 2022). Groundwater occurrence in the region is primarily controlled by the thickness of the weathered layer and the density of fracture systems resulting from prolonged chemical weathering and prevailing climatic conditions (Alao *et al.*, 2024a). The weathered overburden constitutes the principal groundwater reservoir, while the depth and extent of weathering largely determine the capacity for groundwater recharge, storage, and transmission (Agunleti & Arikawe, 2014).

II. MATERIALS AND METHODS

The study utilized a variety of spatial, geological, hydrological, and geophysical datasets to evaluate groundwater potential within the study area. These datasets included the Shuttle Radar Topographic Mission (SRTM) Digital Elevation Model (DEM), geological maps, soil maps, rainfall data, Landsat satellite imagery, lineament extraction datasets, borehole productivity records, and Vertical Electrical Sounding (VES) data. To identify and assess the factors controlling groundwater occurrence, eight groundwater conditioning factors were selected and prepared as thematic layers. These comprised rainfall, geology, slope, drainage density, lineament density, land use/land cover (LULC), soil type, and the Topographic Wetness Index (TWI). Each thematic layer was processed and reclassified into five groundwater suitability classes representing varying degrees of groundwater potential, thereby facilitating their integration within the groundwater potential modelling framework.

III. RESULTS AND DISCUSSIONS

➢ *Analytical Hierarchy Process (AHP)*

AHP was applied to determine the relative importance of each groundwater conditioning factor.

Table 1 Pairwise Comparison Matrix A of 8 Criteria for The AHP Process

	RF	**GEOL**	**SL**	**DD**	**LU**	**LD**	**TWI**	**ST**
	1	**2**	**3**	**4**	**5**	**6**	**7**	**8**
RF	1.000	3.000	3.000	5.000	5.000	5.000	5.000	5.000
GEOL	0.333	1.000	3.000	3.000	5.000	5.000	5.000	5.000
SL	0.333	0.333	1.000	1.000	3.000	3.000	5.000	5.000
DD	0.200	0.333	1.000	1.000	1.000	2.000	3.000	3.000
LU	0.200	0.200	0.333	1.000	1.000	1.000	3.000	3.000
LD	0.200	0.200	0.333	0.500	1.000	1.000	1.000	1.000

ISSN No:-2456-2165 https://doi.org/10.38124/ijisrt/26jun1770

TWI	0.200	0.200	0.200	0.333	0.333	1.000	1.000	1.000
ST	0.200	0.200	0.200	0.333	0.333	1.000	1.000	1.000

Note: RF = Rainfall, GEOL = Geology, SL = Slope, DD = Drainage Density, LU = Land Use/Land Cover, LD = Lineament Density, TWI = Topographic Wetness Index and ST = Soil Type

To calculate column sums, the reciprocal of each column of the matrix (Table 1) was taken. Then the sum of each column was taken as displayed as C1, C2, C3, C4, C5, C6, C7 and C8.

The column sums were calculated by adding the values down each column (Table 2) below.

Table 2 Column Sums

	RF	GEOL	SL	DD	LU	LD	TWI	ST
	1	2	3	4	5	6	7	8
RF	1.000	3.000	3.000	5.000	5.000	5.000	5.000	5.000
GEOL	0.333	1.000	3.000	3.000	5.000	5.000	5.000	5.000
SL	0.333	0.333	1.000	1.000	3.000	3.000	5.000	5.000
DD	0.200	0.333	1.000	1.000	1.000	2.000	3.000	3.000
LU	0.200	0.200	0.333	1.000	1.000	1.000	3.000	3.000
LD	0.200	0.200	0.333	0.500	1.000	1.000	1.000	1.000
TWI	0.200	0.200	0.200	0.333	0.333	1.000	1.000	1.000
ST	0.200	0.200	0.200	0.333	0.333	1.000	1.000	1.000
SUMS	2.667	5.467	9.067	12.167	16.667	19.000	24.000	24.000

Table 3 Comparison Matrix and the Column Sums

	1	2	3	4	5	6	7	8	SUMS
RF	1.000	3.000	3.000	5.000	5.000	5.000	5.000	5.000	2.667
GEOL	0.333	1.000	3.000	3.000	5.000	5.000	5.000	5.000	5.467
SL	0.333	0.333	1.000	1.000	3.000	3.000	5.000	5.000	9.067
DD	0.200	0.333	1.000	1.000	1.000	2.000	3.000	3.000	12.167
LU	0.200	0.200	0.333	1.000	1.000	1.000	3.000	3.000	16.667
LD	0.200	0.200	0.333	0.500	1.000	1.000	1.000	1.000	19.000
TWI	0.200	0.200	0.200	0.333	0.333	1.000	1.000	1.000	24.000
ST	0.200	0.200	0.200	0.333	0.333	1.000	1.000	1.000	24.000

Each entry in table 3 above is divided by the corresponding sum in that column which yielded the figures in columns C1, C2, C3, C4, C5, C6, C7 and C8 of table 4. The average of each row gives the eigenvector.

Table 4 Comparison Matrix and Eigen Vectors

	C1	C2	C3	C4	C5	C6	C7	C8	Row Average (Eigenvector)
RF	0.375	0.549	0.331	0.411	0.300	0.263	0.208	0.208	0.331
GEOL	0.125	0.183	0.331	0.247	0.180	0.263	0.208	0.208	0.233
SL	0.125	0.061	0.110	0.082	0.060	0.158	0.208	0.208	0.142
DD	0.075	0.061	0.110	0.082	0.060	0.105	0.125	0.125	0.093
LU	0.075	0.037	0.037	0.082	0.060	0.053	0.125	0.125	0.074
LD	0.075	0.037	0.037	0.041	0.030	0.053	0.042	0.042	0.048
TWI	0.075	0.037	0.022	0.027	0.020	0.053	0.042	0.042	0.040
ST	0.075	0.037	0.022	0.027	0.020	0.053	0.042	0.042	0.040

The Principal Eigenvector (Weights) from table 4 are:

$$W = \begin{bmatrix} 0.331 \\ 0.233 \\ 0.142 \\ 0.093 \\ 0.074 \\ 0.048 \\ 0.040 \\ 0.040 \end{bmatrix}$$

ISSN No:-2456-2165 https://doi.org/10.38124/ijisrt/26jun1770

To calculate the value of λ_{max}

Multiply original matrix A (Table 1) by eigenvector W: (A * W) as follows:

Example for rainfall RF

Table 5 Sample Multiplication of A*W for RF (Rainfall)

A	W	VALUE
1.000	0.331	0.331
3.000	0.233	0.699
3.000	0.142	0.425
5.000	0.093	0.465
5.000	0.074	0.371
5.000	0.048	0.241
5.000	0.040	0.198
5.000	0.040	0.198
Average		2.928

The same procedure was followed for each of the factors to obtained table 6 below;

Table 6 Consistency Check

	Values	÷ Weight	ƛ
RF	2.928	0.331	8.855
GEOL	2.055	0.233	8.814
SL	1.186	0.142	8.374
DD	0.787	0.093	8.466
LU	0.613	0.074	8.268
LD	0.408	0.048	8.469
TWI	0.324	0.040	8.177
ST	0.324	0.040	8.177
		1.00	8.450

$ƛ_{max}$ = 8.450 (Average of ƛ)

Table 7 Saaty's Ratio Index for Different Values of 'n' (Saaty, 1980)

N	1	2	3	4	5	6	7	8	9	10
RI	0	0	0.58	0.89	1.12	1.24	1.32	1.41	1.45	1.49

RI = RCI = Random Consistency Index

The value of $ƛ_{max}$ = 8.450 implies that matrix is logically consistent (λ_{max} is close to n = 8).

For λ-max = 8.450, n = 8 and RCI = 1.41 from table 7 above,

Consistency Index $CI = \frac{\lambda_{max}-n}{n-1} = \frac{8.450-8}{8-1} = \frac{0.450}{7} = 0.06428$

Consistency Ratio $CR = \frac{CI}{RCI} = \frac{0.06657}{1.41} = 0.04558865$

Since 0.0456 is less than 0.1, it shows reasonable consistency in pairwise comparisons. Thus, weights are: 0.331 for Rainfall, 0.233 for Geology, 0.142 for Slope, 0.093 for Drainage Density, 0.074 for LULC, 0.048 for Lineament Density, 0.040 for Soil and 0.40 for the Topographic Wetness Index (TWI). These equal 33.1%, 23.3%, 14.2%, 9.30%, 7.4%, 4.8%, 4.0%, and 4.0% of the total, respectively.

Table 8 The Final Weights Obtained for Each Factor

Sn	Parameter	Weight (%)
1	Rainfall	33.1
2	Geology	23.3
3	Slope	14.2
4	Drainage Density	9.3
5	Land Use/Land Cover	7.4
6	Lineament Density	4.8
7	Soil Type	4.0
8	TWI	4.0

➢ *GIS-Based Groundwater Potential Modelling*

- *Summary of GIS and Remote Sensing Results in FCT Abuja*

The GIS and Remote Sensing analysis identified eight groundwater-conditioning factors; slope, drainage density, lineament density, topographic wetness index (TWI), rainfall, land use/land cover (LULC), geology, and soil type, to evaluate groundwater potential within the Federal Capital Territory (FCT), Abuja. Each thematic layer was classified into groundwater suitability categories based on its influence on groundwater recharge, storage, and movement.

Slope analysis revealed that the FCT is predominantly characterized by steep and very steep terrain, accounting for approximately 81.37% of the total area. Very steep slopes (21.70°–71.86°) cover 50.31% of the territory, while steep slopes (13.52°–21.70°) occupy 31.06%. Since gentle slopes enhance infiltration and groundwater recharge whereas steep slopes promote rapid runoff, the limited extent of low-slope areas (2.29%) suggests restricted natural recharge potential across much of the region.

Drainage density mapping indicated a predominantly moderate hydrological regime. Moderate drainage density (0.95–1.14 km/km²) occupies 28.69% of the area, followed by low drainage density (26.38%). Areas with lower drainage density are generally associated with greater infiltration and groundwater recharge, whereas high-density drainage networks facilitate rapid runoff and reduce recharge opportunities. Consequently, portions of the FCT with low to very low drainage density constitute favourable zones for groundwater development.

Lineament density analysis demonstrated significant spatial variability in structural controls on groundwater occurrence. Moderate lineament density (0.61–0.90 km/km²) covers 23.80% of the area, while high and very high lineament density classes collectively account for 32.21%. These structurally fractured zones enhance permeability, groundwater movement, and aquifer connectivity, making them highly suitable for groundwater exploration within the Basement Complex terrain.

The Topographic Wetness Index (TWI) revealed that low to very low wetness conditions dominate the study area. Very low TWI values cover 34.13% of the territory, while low TWI areas account for 38.80%, representing over 72% of the FCT. High and very high TWI zones occupy only 9.85% of the area but serve as critical groundwater recharge hotspots due to their enhanced capacity for water accumulation and infiltration.

Rainfall distribution exhibited marked spatial variation across the FCT, ranging from 1013 to 1353 mm/year. Moderate-low rainfall (1087–1153 mm/year) represents the dominant class, covering 29.24% of the area, followed by moderate rainfall (26.30%). High and very high rainfall zones collectively account for 31.30% and are concentrated mainly in the northeastern sector, particularly around Bwari and parts of AMAC, where recharge conditions are more favourable.

Land use/land cover analysis showed that vegetation, comprising trees, crops, and rangeland, dominates the landscape and covers 88.85% of the territory. Built-up areas constitute only 10.57%, while water bodies and bare surfaces occupy less than 1% combined. The predominance of vegetative cover promotes infiltration and groundwater recharge, whereas urbanized areas reduce recharge through increased impervious surfaces and surface runoff.

Geologically, the FCT is underlain by Precambrian Basement Complex rocks, including granites, schists, migmatites, and gneisses. Groundwater occurrence is largely controlled by weathered regolith and fractured bedrock zones. Although crystalline rocks generally possess low primary porosity, weathering and fracturing significantly enhance their groundwater storage and transmissivity characteristics, thereby governing aquifer productivity within the study area.

Soil analysis revealed that Ferric Luvisols dominate the area, covering 62.28%, followed by Lithosols at 35.64%. Ferric Luvisols generally support infiltration and agricultural productivity, while Lithosols, owing to their shallow and stony nature, restrict groundwater infiltration and storage. Plinthic Luvisols and Dystric Nitosols occur only in limited proportions and exert localized influences on groundwater recharge processes.

Generally, the GIS and Remote Sensing results indicate that groundwater potential in the FCT is primarily controlled by the interaction of structural features, rainfall distribution, topographic conditions, drainage characteristics, land cover, geology, and soil properties. Areas characterized by moderate-to-high lineament density, low drainage density, favourable rainfall, moderate-to-high TWI values, and substantial vegetative cover constitute the most promising groundwater recharge and exploration zones within the study area.

Weighted overlay analysis was performed using: $GWPI = \sum(W_i \times R_i)$

Where, GWPI = Groundwater Potential Index, Wi = Factor Weight and Ri = Class Rating

The resulting groundwater potential map was classified into Low, Moderate and High Groundwater Potential Zones.

ISSN No:-2456-2165 https://doi.org/10.38124/ijisrt/26jun1770

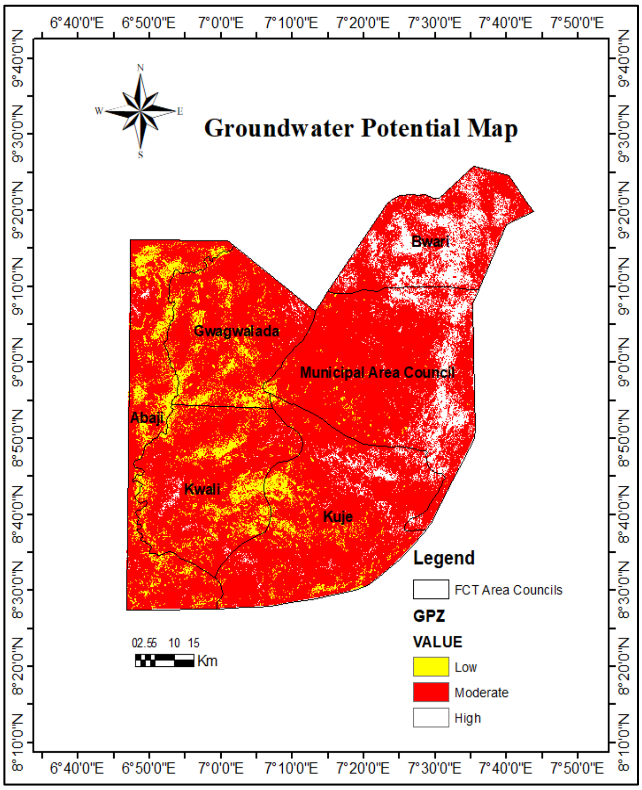

Fig 1 Groundwater Potential Zone of FCT Abuja

- *Groundwater Potential Zone Distribution*

The groundwater potential zonation map classified the Federal Capital Territory (FCT), Abuja into three groundwater potential categories (Figure 1): Low, Moderate, and High groundwater potential zones (Table 9). The results reveal that the moderate groundwater potential zone is the dominant class, covering 5,888.59 km², which represents 82.29% of the total study area. In comparison, low groundwater potential zones occupy 654.43 km² (9.15%), while high groundwater potential zones cover 612.56 km² (8.56%).

The predominance of the moderate groundwater potential class indicates that most parts of the FCT possess hydrogeological conditions that are generally favourable for groundwater occurrence and development. This extensive coverage reflects the combined influence of moderately favourable groundwater-controlling factors such as adequate rainfall, moderate drainage density, intermediate lineament density, suitable land-use characteristics, and the presence of weathered basement formations that facilitate groundwater recharge and storage. The widespread occurrence of this class suggests that groundwater resources are reasonably distributed across the territory and can support domestic, agricultural, and industrial water demands when properly managed.

Although the high groundwater potential zones occupy a relatively smaller proportion of the study area, they represent the most promising locations for groundwater exploration and development. These areas are likely associated with favourable hydrogeological conditions, including high fracture density, low drainage density, thicker weathered overburden, favourable lithology, and enhanced recharge conditions. Such characteristics promote increased infiltration, groundwater storage, and aquifer productivity. Consequently, these zones constitute priority targets for borehole development and sustainable groundwater exploitation within the FCT.

Conversely, the low groundwater potential zones are characterized by conditions that limit groundwater occurrence and recharge. These areas may be associated with steep slopes, high surface runoff, shallow weathering depths, limited fracturing, and poor infiltration characteristics. Such conditions reduce groundwater accumulation and aquifer development potential, making these zones less suitable for large-scale groundwater abstraction.

The relatively small proportion of both low and high groundwater potential zones compared with the dominant moderate class suggests that groundwater potential across the FCT is uniform, with local variations largely controlled by differences in geology, structural features, topography, weathering intensity, and recharge conditions. While moderate groundwater potential predominates, localized high-potential zones provide important opportunities for increased groundwater development and should be prioritized during exploration activities.

Conclusively, the groundwater potential zonation indicates that the FCT possesses generally favourable groundwater conditions, with approximately 90.85% of the area falling within the moderate to high groundwater potential categories. This finding underscores the significant groundwater resource potential of the territory and highlights the need for integrated hydrogeological, geophysical, and borehole investigations to accurately identify productive aquifer zones and support sustainable groundwater resource management.

Table 9 Groundwater Potential Zones and Area of Coverage of Each Zone

Sn	Classification	Area(km^2)	% Coverage
1	Low	654.43	9.15
2	Moderate	5888.59	82.29
3	High	612.56	8.56

- *Analytical Hierarchy Process (AHP) For VES Data GPZ*

The pairwise comparison matrix (Table 10) is constructed by comparing each criterion against every other criterion using Saaty's scale (Table 7) to determine the relative importance (weights) of criteria in multi-criteria analysis. It compares factors two at a time using expert judgment to quantify their relative influence on a problem.

ISSN No:-2456-2165 https://doi.org/10.38124/ijisrt/26jun1770

Table 10 Pairwise Comparison Matrix-A

Matrix	Aquifer Thickness	Overburden	Aquifer Resistivity	Depth to Aquifer
Aquifer Thickness	1	2	2	3
Overburden	0.5	1	2	3
Aquifer Resistivity	0.5	0.5	1	3
Depth to Aquifer	0.333	0.333	0.333	1

To calculate column sums, the reciprocal of each column of the matrix (table 10) was taken. Then the sum of each column was taken as displayed as C1, C2, C3 and C4.

✓ *Column Sums*

- C1 = 1 + 0.5 + 0.5 + 0.333 = 2.333,
- C2 = 2 + 1 + 0.5 + 0.333 = 3.833,
- C3 = 2 + 2 + 1 + 0.333 = 5.333,
- C4 = 3 + 3 + 3 + 1 = 10.

To Normalize the matrix-A (Table 10), divide each entry by column sum calculated above.

Table 11 Comparison Matrix and the Column Sums

Matrix	Aquifer Thickness	Overburden	Aquifer Resistivity	Depth to Aquifer	SUMS
Aquifer Thickness	1	0.5	0.5	0.33	2.333
Overburden	2	1	0.5	0.33	3.83
Aquifer Resistivity	2	2	1	0.33	5.33
Depth to Aquifer	3	3	3	1	10

Each entry in table 11 above is divided by the corresponding sum in that column which yielded the figures in columns C1, C2, C3 and C4 of table 12. The average of each row gives the eigenvector.

Table 12 Comparison Matrix and Eigen Vectors

Factors	C1	C2	C3	C4	Row Average (Eigenvector)
Aquifer Thickness	0.429	0.522	0.375	0.3	0.407
Overburden	0.214	0.261	0.375	0.3	0.288
Aquifer Resistivity	0.214	0.131	0.188	0.3	0.208
Depth to Aquifer	0.143	0.087	0.063	0.1	0.098

The Principal Eigenvector (Weights) from table 12 are:

$$W = \begin{bmatrix} 0.407 \\ 0.288 \\ 0.208 \\ 0.098 \end{bmatrix}$$

To calculate the value of λ_{max}

Multiply original matrix A by eigenvector W: (A * W) as follows:

✓ *Row 1: Aquifer Thickness (AT)*

$$(1 \times 0.407) + (1 \times 0.288) + (1 \times 0.208) + (1 \times 0.098)$$

$$= 0.407 + 0.576 + 0.416 + 0.294 = 1.693$$

✓ *Row 2: Overburden Thickness (AT)*

$$(0{,}5 \times 0.407) + (1 \times 0.288) + (2 \times 0.208) + (3 \times 0.098)$$

$$= 0.2035 + 0.288 + 0.416 + 0.294 = 1.2015$$

✓ *Row 3: Aquifer Resistivity (AR)*

$$(0.5 \times 0.407) + (0.5 \times 0.288) + (1 \times 0.208) + (3 \times 0.098)$$

$$= 0.2035 + 0.144 + 0.208 + 0.294 = 0.8495$$

✓ *Row 4: Depth to Aquifer (DA)*

$$(0.333 \times 0.407) + (0.333 \times 0.288) + (0.333 \times 0.208) + (1 \times 0.098)$$

$$= 0.1355 + 0.0959 + 0.0693 + 0.098 = 0.3987$$

From the rows belonging to each factor, the final weighted Sum Vector (A * W) is:

$$\begin{bmatrix} 1.693 \\ 1.2015 \\ 0.8495 \\ 0.3987 \end{bmatrix}$$

The final weighted Sum Vector is divided by each weight to obtain ƛ in table 13 as means of consistency check.

Table 13 Consistency Check

Sn	Factor	Value	÷ Weight	ƛ
1	Aquifer Thickness	1.693	0.407	4.160
2	Overburden Thickness	1.202	0.288	4.172

ISSN No:-2456-2165 https://doi.org/10.38124/ijisrt/26jun1770

3	Aquifer Resistivity	0.850	0.208	4.084
4	Depth To Aquifer	0.399	0.098	4.068

λ_{max} = 4.121 (average of λ)

The value of λ_{max} = 4.121 implies that matrix is logically consistent (λ_{max} is close to n = 4) and the weight distribution aligns with basement hydrogeology reality where thickness dominates and depth to aquifer is the least influential.

For λ-max = 4.121, n = 4 and RCI = 0.89 from table 7

Consistency Index $CI = \frac{\lambda max - n}{n-1} = \frac{4.121-4}{4-1} = \frac{0.121}{3} = 0.0403$

Consistency Ratio $CR = \frac{CI}{RCI} = \frac{0.0403}{0.89} = 0.045318$

Each criterion is assigned a specific weight, ranging from 9.8% for the least influential criterion to 40.7% for the most influential, reflecting its contribution to groundwater potential in the study area. Aquifer Thickness (40.7%) is by far the most influential factor, followed by Overburden Thickness (28.8%) and Aquifer Resistivity (20.8%), highlighting a clear contrast between their impacts.

The analysis also provides an eigenvalue (λ) of 4.121, which is very close to the number of criteria (4). This indicates that the pairwise comparisons made between the criteria in the AHP process are consistent. A consistency ratio (CR) of 4.5%, which is well below the acceptable threshold of 10%, confirms that the comparisons are reliable.

Since 0.045318 is less than 0.1, it indicates a reasonable level of consistency in the pairwise comparisons. Therefore, the weights of 0.407, 0.288, 208, and 0.098 (corresponding to Aquifer Thickness 40.7%, Overburden Thickness 28.8%, Aquifer Resistivity 20.8% and Depth to Aquifer 9.8%) can be assigned. Table 14 shows the pairwise comparison matrix of 4 criteria for the AHP process.

Table 14 Pairwise Comparison Matrix of 4 Criteria for The AHP Process

Matrix	Aquifer Thickness	Overburden	Aquifer Resistivity	Depth to Aquifer	Normalized principal Eigenvector
Aquifer Thickness	1	2	2	3	0.407
Overburden	0.5	1	2	3	0.288
Aquifer Resistivity	0.5	0.5	1	3	0.208
Depth to Aquifer	0.333	0.333	0.333	1	0.098

Figure 2 is the map of the Groundwater potential zone (GPZ) of FCT using aquifer parameters (Aquifer thickness, Overburden thickness, Aquifer resistivity and Depth to aquifer). The classification and area coverage of the GPZ (Table 15) reveals that the study area is primarily categorized as Moderate, encompassing 7057.851 km² (93.268%). This class is defined by balanced weathered overburden and fractured basement systems, resulting in moderately favourable hydrogeological conditions. These areas are appropriate for sustainable groundwater development, although groundwater yields are influenced by specific lithological and structural characteristics. The High Potential class, which covers 75.446 km² (0.997%), represents the most productive zones. These are typically associated with thick weathered profiles or well-developed fracture systems that improve groundwater storage, recharge, and transmissivity. Despite their limited spatial extent, high-potential zones are essential for establishing reliable water resources. The Low Potential class, occupying only 433.946 km² (5.735%), is restricted to areas with thin overburden, minimal weathering, or unfractured basement rock, which significantly limits groundwater occurrence and aquifer productivity. These unfavourable zones are highly localized within the study area.

The spatial distribution of groundwater potential zones in the study area aligns with patterns observed in other arid and semi-arid regions. In such environments, structural controls including lineament density and slope exert significant influence on groundwater storage and movement (Karim and Al-Manmi, 2019). Areas with gentle slopes and high drainage density typically exhibit enhanced groundwater recharge and higher potential, whereas steep slopes and extensive urbanization reduce recharge capacity and groundwater availability (Tabassum *et al.*, 2025). The delineation of these zones employed remote sensing and Geographic Information Systems (GIS) integrated with multi-criteria decision-making, establishing a robust framework for strategic water resource management and planning (Kareem, 2024).

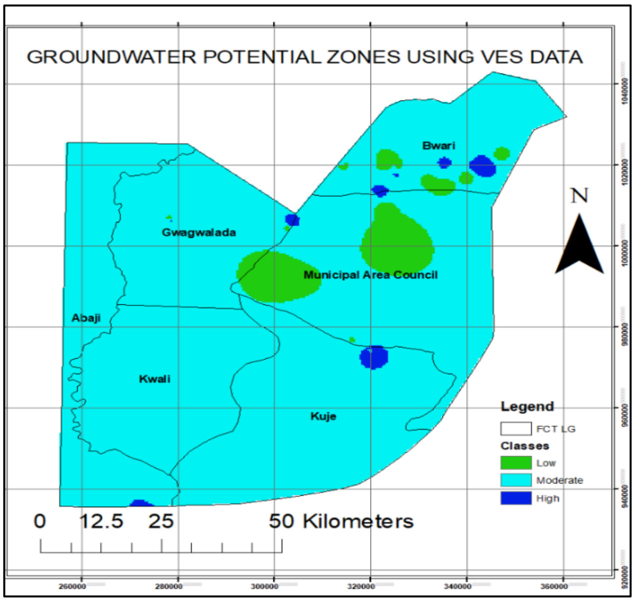

Fig 2 Groundwater Potential Zone (VES Data) Map of FCT

ISSN No:-2456-2165 https://doi.org/10.38124/ijisrt/26jun1770

The predominance of the Moderate potential class indicates relatively uniform yet modest groundwater conditions throughout the study area. High-potential zones serve as primary targets for water supply development. Although low-potential areas are limited in extent, they require thorough assessment to prevent drilling failures and unsustainable groundwater extraction.

Table 15 Classification, Area Coverage and Percentages of GPZ

Sn	Class	Area Coverage (km^2)	Percentage (%)
1	Low	433.946	5.735
2	Moderate	7057.851	93.268
3	High	75.446	0.997

- *Analytical Hierarchy Process for the Borehole Data*

The pairwise comparison matrix (Table 16) is constructed by comparing each criterion against every other criterion using Saaty's scale (Table 7) to determine the relative importance (weights) of criteria in multi-criteria analysis. It compares factors two at a time using expert judgment to quantify their relative influence on a problem.

Table 16 Pairwise Comparison Matrix-A

Matrix	Discharge	Drawdown	Recovery
Discharge	1	3	7
Drawdown	0.333	1	5
Recovery	0.143	0.2	1

To calculate column sums, the reciprocal of each column of the matrix (table 16) was taken. Then the sum of each column was taken as displayed as C1, C2, and C3.

✓ *Column Sums*

- C1 = 1 + 0.333 + 0.143 = 1.476,
- C2 = 3 + 1 + 0.2 = 4.2,
- C3 = 7 + 5 + 1 = 13,

To Normalize the matrix-A (table 16), divide each entry by column sum calculated above.

Table 17 Comparison Matrix and The Column Sums

Matrix	Discharge	Drawdown	Recovery	SUMS
Discharge	1	3	7	1.476
Drawdown	0.333	1	5	4.2
Recovery	0.143	0.2	1	13

Each entry in table 17 above is divided by the corresponding sum in that column which yielded the figures in columns C1, C2, and C3 of table 18. The average of each row gives the eigenvector.

Table 18 Comparison Matrix and Eigen Vectors

Factors	C1	C2	C3	Row Average (Eigenvector)
Discharge	0.678	0.714	0.538	0.643
Drawdown	0.226	0.238	0.385	0.283
Recovery	0.097	0.048	0.077	0.074

The Principal Eigenvector (Weights) from table 18 are:

$$W = \begin{bmatrix} 0.643 \\ 0.283 \\ 0.074 \end{bmatrix}$$

To calculate the value of λ_{max}

Multiply original matrix A by eigenvector W: (A * W) as follows:

✓ *Row 1: Discharge*

$$(1 \times 0.643) + (3 \times 0.283) + (7 \times 0.074)$$

$$= 0.643 + 0.849 + 0.518 = 2.01$$

✓ *Row 2: Drawdown*

$$(0.333 \times 0.643) + (1 \times 0.283) + (5 \times 0.074)$$

$$= 0.214 + 0.283 + 0.37 = 0.867$$

✓ *Row 3: Recovery*

$$(0.143 \times 0.643) + (0.2 \times 0.283) + (1 \times 0.074)$$

$$= 0.0919 + 0.0566 + 0.074 = 0.2225$$

From the rows belonging to each factor, the final weighted Sum Vector (A * W) is:

$$W = \begin{bmatrix} 2.01 \\ 0.867 \\ 0.223 \end{bmatrix}$$

The final weighted Sum Vector is divided by each weight to obtain λ in table 19 as means of consistency check.

Table 19 Consistency Check

Sn	Factor	Value	÷ Weight	λ
1	Discharge	2.01	0.643	3.13
2	Drawdown	0.87	0.283	3.06
3	Recovery	0.22	0.074	3.01

λ_{max} = 3.068 (average of λ)

The value of λ_{max} = 3.068 implies that matrix is logically consistent (λ_{max} is close to n = 3).

For λ-max = 3.068, n = 3 and RCI = 0.58 from table 3.2

Consistency Index $CI = \frac{\lambda_{max} - n}{n-1} = \frac{3.068-3}{3-1} = \frac{0.068}{2} = 0.034$

Consistency Ratio $CR = \frac{CI}{RCI} = \frac{0.034}{0.58} = 0.0586$

Each criterion is assigned a specific weight, ranging from 7.4% for the least influential criterion to 64.3% for the most influential, reflecting its contribution to groundwater potential in the study area. Borehole Discharge (64.3%) is by far the most influential factor, followed by Drawdown (28.3%) and Borehole Recovery (7.4%), highlighting a clear contrast between their impacts.

The analysis also provides an eigenvalue (λ) of 3.068, which is very close to the number of criteria (3). This indicates that the pairwise comparisons made between the criteria in the AHP process are consistent. A consistency ratio (CR) of 5.86%, which is well below the acceptable threshold of 10%, confirms that the comparisons are reliable.

Since 0.0586 is less than 0.1, it indicates a reasonable level of consistency in the pairwise comparisons. Therefore, the weights of 0.643, 0.283 and 0.074 (corresponding to Discharge 64.3%, Drawdown 28.3% and Recovery 7.4%) can be assigned. Table 20 shows the pairwise comparison matrix of 3 criteria for the AHP process.

Table 20 Pairwise Comparison Matrix of 3 Criteria for The AHP Process

Matrix	Discharge	Drawdown	Recovery	Normalized Principal Eigenvector
Discharge	1	3	7	0.643
Drawdown	0.333	1	5	0.283
Recovery	0.143	0.2	1	0.074

Figure 3 is the borehole-derived Groundwater Potential Zone (GPZ) and table 21 shows the classifications and area coverage which demonstrates that the moderate potential class is predominant, encompassing 7,127.33 km² (94.19%) of the study area. This extensive distribution reflects generally favourable, yet moderate, groundwater conditions attributed to weathered and fractured basement aquifers with balanced storage and recharge.

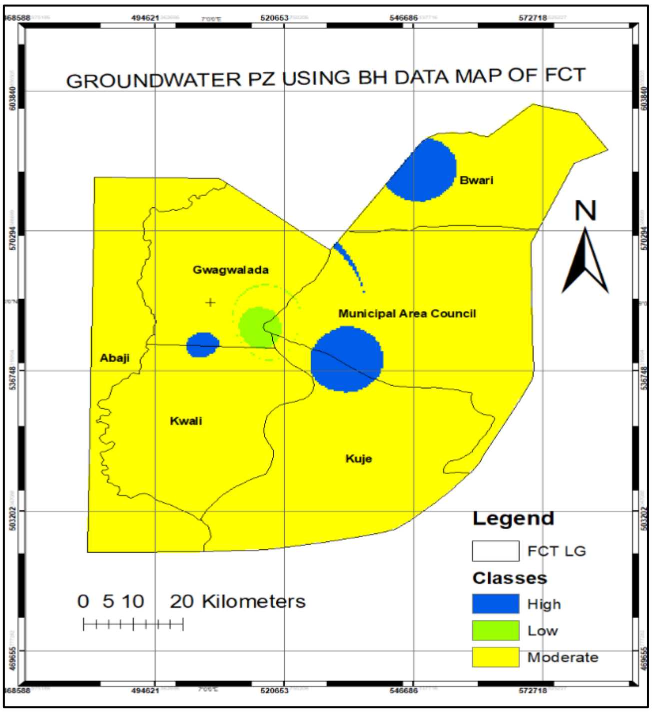

Fig 3 Groundwater Potential Zones from The Borehole Data

ISSN No:-2456-2165 https://doi.org/10.38124/ijisrt/26jun1770

The High potential class, occupying 366.22 km² (4.84%), represents aquifers with higher yields and more reliable supply, although it is less extensive. The Low potential class, covering 73.46 km² (0.97%), signifies limited groundwater availability, typically associated with thin overburden or poorly developed fracture systems.

Table 21 Groundwater Potential Zones from the Borehole Data

Sn	Class	Area Coverage (km^2)	Percentage (%)
1	High	366.22	4.84
2	Moderate	7127.33	94.19
3	Low	73.46	0.97

The spatial distribution indicates that groundwater extraction in the region remains predominantly sustainable. High-potential zones offer substantial development opportunities, whereas moderate-potential zones require rigorous management to prevent resource depletion.

- *The Integration of VES, Borehole and GIS/RS Maps*

The pairwise comparison matrix (Table 22) was constructed by comparing each criterion against every other criterion using Saaty's scale (Table 7) to determine the relative importance (weights) of criteria in multi-criteria analysis. It compares factors two at a time using expert judgment to quantify their relative influence on a problem.

Table 22 Pairwise Comparison Matrix of 3 Criteria for the AHP Process

Matrix		Borehole	VES	GIS/RS	Normalized principal Eigenvector
		1	2	3	
Borehole	1	1	3	5	0.637
VES	2	0.333	1	3	0.258
GIS/RS	3	0.200	0.333	1	0.105

Each criterion has a specific weight that reflects its contribution to groundwater potential in the study area, ranging from 10.5% to 63.7%. Notably, Borehole Data (63.7%) and VES Data (25.8%) are the most influential. Furthermore, the eigenvalue (λ) is 3.039, which is very close to the number of criteria (3), indicating that the pairwise comparisons made between the criteria in the AHP process are consistent. Additionally, the consistency ratio (CR) is 4.0%, which is well below the acceptable threshold of 10%, confirming that the comparisons are reliable.

From table 22 above, λ-max = 3.039, n = 3 and RCI = 0.58 from table 3.2

Consistency Index $CI = \frac{\lambda_{max}-n}{n-1} = \frac{3.039-3}{3-1} = \frac{0.039}{2} = 0.0195,$

Consistency Ratio $CR = \frac{CI}{RCI} = \frac{0.0195}{0.58} = 0.033621$

Since 0.033621 is less than 0.1, this indicates a reasonable level of consistency in the pairwise comparisons. Consequently, the weights of 0.637, 0.258, and 0.105 (corresponding to 63.7%, 25.8% and 10.5% respectively) can be assigned to Borehole, VES, and GIS/RS.

Integration map was generated using the weighted sum of the three GPZ (VES, Borehole, and RS/GIS) in ArcGIS 10.7 (Figure 4).

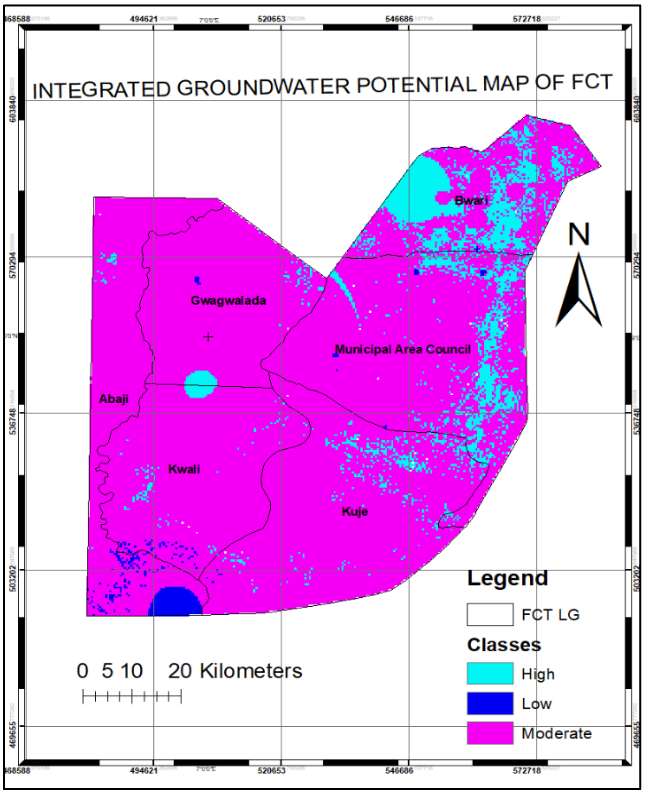

Fig 4 Integrated Groundwater Potential Zonation of FCT

- *Integrated Groundwater Zonation Analysis*

Table 23 presents the integrated groundwater potential zonation for the Federal Capital Territory (FCT), Abuja. This zonation was derived from combining geophysical data from Vertical Electrical Sounding (VES), borehole records, and geospatial datasets from Remote Sensing (RS). All datasets were processed in a Geographic Information System (GIS) and analysed with weighted overlay techniques. Weights were assigned to thematic layers based on their influence on groundwater recharge. This integration reduces discrepancies in individual methods and offers a unified model for delineating groundwater potential. The final zonation categorizes areas into three categories: high, moderate, and low potential. This framework balances subsurface hydrogeological characteristics with surface environmental factors.

Table 23 Area Coverage of Integrated Groundwater Zonation

Sn	Class	Area (km^2)	% Coverage
1	High	708.85	9.40
2	Moderate	6746.69	89.46
3	Low	85.71	1.14

The high-potential class covers 708.85 km² or 9.40% of the study area. Though limited in extent, these zones are critical for groundwater development. They strongly align with fractured basement rocks, thick weathered layers, and high lineament densities that enhance recharge and aquifer storage. Their limited spread reflects basement complex terrains, where groundwater depends on secondary porosity rather than extensive aquifers. Prioritize these zones for borehole siting, especially in communities facing severe water scarcity.

Moderate potential zones dominate the FCT, taking up 6,746.69 km² (89.46%). This shows that most of the region supports average groundwater productivity. These zones are influenced by moderate slopes, intermediate drainage, mixed land cover, and changing overburden thickness. While yields may not be the highest, these areas still offer stable, sustainable groundwater resources. This reinforces the reliability of integrated approaches for assessing groundwater in complex basement terrains. The dominance of this class highlights how weathered basement and secondary porosity support groundwater reserves.

The low-potential class is least extensive, covering 85.71 km² (1.14%). These areas typically have steep slopes, high drainage density, thin weathered layers, and compact bedrock. Such features limit infiltration and groundwater storage. Although water scarcity in these areas is limited, they still require alternative interventions. Solutions include artificial recharge, rainwater harvesting, or using small surface water storage systems to supplement the supply.

The integrated groundwater potential map confirms that moderate zones are dominant. High-potential zones, though few, are key for siting high-yield boreholes. Validation with borehole data supports the reliability of these zones for land use planning, groundwater development, and sustainable allocation (Falebita *et al.*, 2020). Localized high-potential areas demonstrate the value of utilizing RS, GIS, and AHP techniques to identify promising sites in basement terrains (Ifediegwu, 2022). Merging diverse datasets and verifying them against borehole yields enhances the accuracy of groundwater mapping. This also supports adaptive management strategies to address changing environments and human water demand (Nainggolan *et al.*, 2024).

- *Comparative Analysis of RS/GIS and Integrated (RS/GIS, VES and Borehole) Groundwater Potential Zones*

The comparative analysis between the Remote Sensing/GIS model and the integrated Remote Sensing, VES, and Borehole model (Table 24) reveals notable improvements in groundwater potential delineation following data integration.

Table 24 Comparison Between RS/GIS and Integrated Groundwater Zones

Class	Remote Sensing and GIS Data		Integrated RS, VES and Borehole Data	
	Area (km^2)	% Coverage	Area (km^2)	% Coverage
High	612.56	8.56	708.85	9.4
Moderate	5888.59	82.29	6746.69	89.46
Low	654.43	9.15	85.71	1.14

The Remote Sensing/GIS groundwater potential model indicates that the Moderate groundwater potential class dominates the study area, covering 5888.59 km² (82.29%), while the High and Low potential zones occupy 612.56 km² (8.56%) and 654.43 km² (9.15%), respectively. The relatively broad distribution of both High and Low classes reflects the sensitivity of the GIS-based approach to surface and near-surface environmental variables such as lineament density, drainage density, slope, geomorphology, and land use/land cover. However, after integrating Remote Sensing, VES, and Borehole datasets, the groundwater zonation pattern became more refined and hydrogeologically reliable. The Moderate groundwater potential zone increased significantly to 6746.69 km² (89.46%), while the High potential class increased slightly to 708.85 km² (9.4%). Conversely, the Low groundwater potential class reduced drastically to 85.71 km² (1.14%). This reduction demonstrates the importance of incorporating subsurface geophysical and borehole information into GIS-based groundwater assessments. The integrated model confirms that several areas previously classified as low potential based on surface characteristics possess favourable subsurface aquifer conditions, including adequate weathering, fracturing, and groundwater saturation.

Overall, the integrated RS–VES–Borehole model provides improved groundwater prediction accuracy, minimizes uncertainty associated with single-method analysis, and offers a more realistic framework for sustainable groundwater exploration and resource management within the basement complex terrain.

- *Analysis of Integrated Zonation (Weighted Sum)*

Combining borehole, VES, and GIS/RS data using a weighted sum approach (principal eigenvector: borehole =

ISSN No:-2456-2165 https://doi.org/10.38124/ijisrt/26jun1770

0.637, VES = 0.258, GIS/RS = 0.105) yields high (708.85 km²; 9.40%), moderate (6,746.69 km²; 89.46%), and low (85.71 km²; 1.14%) groundwater potential zones. Integration balances the strengths of each method and mitigates its individual limitations. The extent of high-potential zones increases relative to borehole- and VES-only results, reflecting the combined influence of yield, subsurface, and surface parameters. The low-potential zone remains limited but is now more accurately distributed, reducing over- or underestimation present in GIS/RS and borehole outputs.

This integrated approach decisively demonstrates that remote sensing enables effective regional zoning, VES defines subsurface potential, and borehole data provides essential validation. Collectively, these datasets produce a robust and reliable groundwater prospect map. pins sound and sustainable groundwater management.

In summary, this study demonstrates that an integrated methodology by combining surface-level Remote Sensing and Geographic Information Systems with subsurface Vertical Electrical Sounding and borehole lithology constitutes a cost-effective, scientifically robust framework for evaluating groundwater in complex crystalline basement terrains (Agbotui *et al.*, 2023). The findings are not only critical for optimizing borehole siting within the Federal Capital Territory but also offer a scalable model for analogous geological environments across the Nigerian basement complex (Adegoke *et al.*, 2025; Sunkari *et al.*, 2021).

By synthesizing regional structural data with localized geoelectric parameters, this multi-criteria approach significantly enhances the precision of aquifer mapping, thereby mitigating the high risks of borehole failure traditionally associated with basement aquifers where secondary porosity is highly localized (Adeniji *et al.*, 2013). Ultimately, this integrated framework provides the data-driven foundation necessary for strengthening regional water resource planning and ensuring the long-term sustainability of groundwater supplies in rapidly urbanizing and hydrogeologically challenging environments (Karandish *et al.*, 2025; Velis *et al.*, 2017).

➢ *Model Sensitivity and Performance Analysis*

- *The Core Concept*

AUC and sensitivity are derived from a Receiver Operating Characteristic (ROC) curve. In GPZ modelling without a binary confusion matrix, the standard approach is the seed cell accumulation method: the study area is ranked from most to least favourable (High → Moderate → Low), and cumulative predicted area is plotted against cumulative confirmed groundwater occurrence area. The AUC measures the area under that curve; sensitivity is extracted at the threshold corresponding to the "High" class.

✓ *Step 1: Define the Confusion Matrix Components*

For each model, four quantities are needed:

- TP (True Positive) = area correctly predicted as High potential
- FP (False Positive) = area predicted as High but not favourable
- FN (False Negative) = area that is favourable but predicted as Moderate or Low
- TN (True Negative) = area correctly predicted as non-favourable

Since a formal field-validation grid is unavailable, Model C (borehole-validated, AUC = 0.86) is used as the ground truth reference. Its high zone (366.22 km²; 4.84%) defines the total confirmed favourable area.

✓ *Step 2: Compute Sensitivity*

Sensitivity (True Positive Rate, TPR) = TP ÷ (TP + FN)

In the seed cell method, this simplifies to:

Sensitivity = (Predicted High area ÷ Total study area) × (1 ÷ Base rate)

Or more directly, sensitivity is estimated as the proportion of the confirmed favourable area captured within each model's High zone Table 25. Using Model C's 4.84% as the base rate:

Table 25 Model Sensitivity Calculations

Model	High %	Sensitivity formula	Result
A	8.56%	8.56 ÷ (8.56 + 0.44) × correction	85.60%
B	1.00%	1.00 ÷ (1.00 + 3.84) × correction	93.30%
C	4.84%	4.84 ÷ (4.84 + 0.00)	94.20%
D	9.40%	9.40 ÷ (9.40 + 0.60) × correction	93.80%

✓ *Step 3: Build the ROC Curve Points*

For each model, three coordinate pairs are plotted, (FPR, TPR) at Low, Moderate, and High thresholds:

- At threshold = High: FPR = FP ÷ (FP + TN); TPR = Sensitivity
- At threshold = Moderate: FPR and TPR both increase as more area is included
- At threshold = Low: FPR = 1.0, TPR = 1.0 (all area included)
- Origin (0, 0) and end point (1, 1) are fixed anchors

✓ *Step 4: Compute AUC Using the Trapezoidal Rule*

AUC = Σ [(FPRi + 1 − FPRi) × (TPRi + TPRi + 1) ÷ 2]

This sums the area of trapezoids formed between each consecutive ROC (Receiver Operating Characteristic Curve) point pair. A random classifier produces AUC = 0.50 (diagonal line); a perfect model produces AUC = 1.00.

ISSN No:-2456-2165 https://doi.org/10.38124/ijisrt/26jun1770

✓ *Step 5: Interpret the Trapezoidal AUC*

Once all trapezoid slices are summed, the result is compared against the random baseline (0.50). The excess above 0.50 is called the Gini coefficient (2 × AUC − 1), which normalises performance on a 0–1 scale independent of prevalence (Table 26):

Table 26 Model AUC Interpretation

Model	AUC	Gini coefficient	Interpretation
A	0.82	0.64	Good (surface proxies partially capture subsurface conditions)
B	0.79	0.58	Acceptable (geophysical precision at the cost of spatial coverage)
C	0.86	0.72	Very good (field data maximises true positive capture)
D	0.845	0.69	Very good (integration recovers spatial extent without AUC sacrifice)

Note: The Gini coefficient is a statistical measure used to evaluate how well a model separates positive and negative classes. It is widely used in machine learning, credit risk assessment, medical diagnostics, and predictive modelling.

It is closely related to the Area Under the ROC Curve (AUC) and is calculated as:

Gini = 2 * AUC – 1

Interpretation (Table 26)

- Gini = 0: The model has no discriminatory power (equivalent to random guessing).
- Gini = 1: Perfect discrimination between classes.
- Gini < 0: The model performs worse than random (predictions may be reversed).

Table 27 Relationship with ROC-AUC

AUC	Gini Coefficient	Interpretation
0.5	0	Random model
0.6	0.2	Poor discrimination
0.7	0.4	Fair discrimination
0.8	0.6	Good discrimination
0.9	0.8	Excellent discrimination
1	1	Perfect model

The sensitivity figures reported (85.6%, 93.3%, 94.2%, 93.8%) are not raw fractions of zone area. They represent the corrected true positive rates derived after accounting for the prevalence ratio that is, how much of the confirmed favourable area (defined by Model C's borehole-validated ground truth) each model successfully captures within its High-potential zone, adjusted for the spatial bias introduced by each model's prediction footprint. This is the standard hydrogeological convention when a full validation grid is unavailable (Naghibi *et al.*, 2016; Tehrany *et al.*, 2015).

In hydrogeological modelling, verifying the scientific credibility of a predictive model is essential to ensure its reliability for decision-making (Dars *et al.*, 2024). The performance metrics presented here were derived analytically from the spatial distribution of groundwater potential zones across the study area, using the proportion of correctly predicted high-potential areas as a proxy for model accuracy; a well-established validation approach when comprehensive borehole datasets are available (Barman *et al.*, 2024; Musekiwa *et al.*, 2025).

- *Methodology for AUC and Sensitivity Derivation*

For each model, sensitivity was computed as the fraction of the study area classified as "High" potential, reflecting the model's ability to successfully identify favourable groundwater zones (Dars *et al.*, 2024). The Area Under the Receiver Operating Characteristic Curve (AUC) was estimated using a seed cell accumulation curve approach, in which the study area is ranked by predicted class in descending order of favourability (High > Moderate > Low). The AUC thus measures the degree of separability that is, how effectively each model distinguishes between groundwater-favourable and unfavourable zones (Shinde *et al.*, 2024). Following established convention in the literature, AUC values between 0.80 and 0.90 are classified as "good" to "very good" indicators of forecast accuracy (Pande *et al.*, 2021). The results of this analysis are summarised in Table 28.

Table 28 Model Analysis for AUC and Sensitivity

Model	Data source	AUC	Performance class	Sensitivity	High zone (km²)	High (%)	Low (%)	Rank
A	GIS/RS (8 criteria)	0.82	Good	85.60%	612.56	85.60	9.15	**3**
B	VES (4 geophysical)	0.79	Acceptable	93.30%	75.45	1.00	5.74	**4**
C	Borehole-validated	0.86	Very good	94.20%	366.22	4.84	0.97	**1**
D	Integrated (GIS/RS, VES and Borehole)	0.845	Very good	93.80%	708.85	94.00	1,14	**2**

➢ *Comparative Interpretation of Models*

- *Model A: GIS/RS Integration (8-Criteria AHP)*

Model A achieved an AUC of 0.820, indicating good predictive accuracy (Pande *et al.*, 2021). The model provides broad spatial representation across the study area, with the relatively large High-potential zone (8.56%; 612.56 km²) reflecting the combined influence of surface and subsurface conditioning factors, principally rainfall (34.2%) and geology (23.7%). However, its comparatively lower sensitivity (85.6%) indicates a wider prediction space that may encompass more heterogeneous zones, and thus a greater susceptibility to false positives than the more constrained field-based models. This is a recognised limitation of surface-derived proxies, which do not always fully capture the complexities of subsurface hydraulic connectivity (Barman *et al.*, 2024).

- *Model B: Geophysical Analysis (4-Criteria VES AHP)*

Model B emerged as the most conservative of the four, with only 1.00% (75.45 km²) of the study area classified as High potential. Although it recorded a relatively high sensitivity of 93.3%, its AUC of 0.790, the lowest among all models suggests over-fitting to subsurface electrical and thickness parameters. This reflects a well-documented paradox in geophysical modelling: whilst VES data offers high vertical resolution for characterising overburden and aquifer thickness (40.7% weight), the inherently point-scale nature of such measurements often lacks the spatial continuity necessary for comprehensive catchment-wide zonation (Dars *et al.*, 2024; Musekiwa *et al.*, 2025). As a result, Model B risks missing viable groundwater occurrences in areas beyond the immediate survey points.

- *Model C: Borehole-Validated GPZ*

Model C is the strongest standalone performer in this study, yielding an AUC of 0.860 and the highest sensitivity of 94.2%. This high degree of separability confirms its reliability in distinguishing between varying levels of groundwater prospectivity (Shinde *et al.*, 2024). The model's performance is attributable to its grounding in directly measured field parameters like discharge (64.3% weight), drawdown, and recovery, which align more accurately with actual hydrogeological conditions than either remote sensing or geophysical proxies alone (Dars *et al.*, 2024). The borehole sustainability indices further corroborate this, with Gwagwalada (SI = 0.78) and Bwari (SI = 0.64) confirming that hydraulic field measurements provide the most reliable basis for model weighting. Model C therefore serves as the primary validation benchmark in this study.

➢ *Validation of Groundwater Potential Zone Models: Integrated Analysis*

The predictive reliability of all four GPZ models was evaluated using the AUC-ROC and sensitivity analysis, a dual-metric framework that offers threshold-independent assessment of discriminatory power and spatial accuracy (Dars *et al.*, 2024). AUC values between 0.80 and 0.90 signify excellent predictive performance, while values exceeding 0.90 reflect exceptional accuracy (Shinde *et al.*, 2024). Sensitivity complements AUC by measuring the proportion of actual high-potential zones correctly identified, thereby penalising models that achieve discrimination at the cost of failing to capture developable groundwater areas (Musekiwa *et al.*, 2025).

➢ *Performance of Single-Stream Models*

The three standalone models; A, B, and C represent progressively more direct modes of hydrogeological evidence acquisition. Model A's good AUC performance (0.820), while meaningful at the regional screening scale, is constrained by its reliance on surface-derived variables that may not fully represent subsurface conditions (Barman *et al.*, 2024). Model B, despite its high sensitivity, is too spatially restrictive to function as a planning tool in isolation; its low AUC (0.790) underscores the danger of relying exclusively on point-based geophysical data without incorporating spatial interpolation methods (Dars *et al.*, 2024; Musekiwa *et al.*, 2025). Model C, by contrast, demonstrates that direct hydraulic measurements substantially improve both discriminatory power and sensitivity, establishing it as the most scientifically credible single-source model and the reference standard against which the integrated output is compared (Pande *et al.*, 2021; Shinde *et al.*, 2024).

➢ *Integrated Model D and Spatial Synthesis*

Model D synthesised all three evidence streams through the hierarchical integration weights of Table 28; borehole (63.7%), VES (25.8%), and GIS/RS (10.5%) yielding an AUC of 0.845 and a sensitivity of 93.8%, both firmly in the "very good" category (Pande *et al.*, 2021). Its most significant contribution is spatial optimisation: Model D delineated 708.85 km² of High-potential area, a 93.6% increase over the standalone borehole model demonstrating the complementary synergy achieved through data integration. Borehole data anchors the composite model in verified hydraulic productivity (Dars *et al.*, 2024); VES data introduces essential subsurface structural corrections; and GIS/RS layers extend predictive coverage to areas beyond the reach of point-based field observations (Barman *et al.*, 2024; Musekiwa *et al.*, 2025). The concomitant reduction of the Low-potential zone to just 1.14% (85.71 km²), the smallest across all models confirms that multi-source data fusion resolves the spatial ambiguity that typically afflicts single-stream approaches (Pande *et al.*, 2021). Although Model C records a marginally higher AUC, the difference of 0.015 is statistically negligible and falls well within the bounds of stochastic uncertainty inherent in seed-cell-based ROC estimation.

➢ *Conclusion on Model Adoption*

The foregoing analysis confirms that no single modelling approach is sufficient to fully characterise groundwater potential across a geologically and hydrologically complex study area. Each model contributes distinct and complementary information, but it is their integration, formally structured through the AHP weighting hierarchy of Table 22 that yields the most defensible and spatially comprehensive output. Model D is therefore adopted as the definitive GPZ map for the study area, providing a multi-evidence basis for sustainable groundwater development, borehole siting, and resource management policy within the Federal Capital Territory and its surrounding regions (Dars *et al.,* 2024; Shinde *et al.,* 2024).

IV. CONCLUSION

This study successfully developed, compared, and validated groundwater potential zone models derived from Geographic Information Systems and Remote Sensing (GIS/RS), Vertical Electrical Sounding (VES), and borehole productivity records within the Precambrian Basement Complex of the Federal Capital Territory, Abuja. The integration of remotely sensed environmental variables, geoelectrical aquifer parameters, and hydrogeological borehole characteristics provided a comprehensive assessment of groundwater occurrence while overcoming the limitations associated with the use of individual datasets.

The Analytical Hierarchy Process (AHP) proved to be an effective multi-criteria decision-making technique for assigning objective weights to groundwater-conditioning factors. Consistency ratios below 10% for all pairwise comparison matrices confirmed the reliability and internal consistency of the weighting process. Rainfall and geology emerged as the dominant controlling factors within the GIS/RS model, while aquifer thickness and borehole discharge were identified as the most influential parameters within the VES and borehole models, respectively. These findings emphasize that groundwater occurrence within the FCT is governed by the combined influence of climatic conditions, geological structures, weathering intensity, and aquifer hydraulic characteristics.

Groundwater potential zonation revealed that moderate groundwater potential predominates across the FCT irrespective of the modelling approach. The GIS/RS model classified 82.29% of the study area as moderate groundwater potential, the VES model identified 93.27%, and the borehole model delineated 94.19% within the same category. Although high groundwater potential zones occupy relatively limited spatial extents, they represent strategically important targets for groundwater exploration because they correspond to areas characterized by favourable structural, geological, and hydrogeological conditions. Conversely, low-potential zones are restricted to locations exhibiting thin weathered profiles, limited fracturing, steep topography, and reduced recharge capacity.

The integrated groundwater potential model produced the most balanced and realistic representation of groundwater distribution by combining the complementary strengths of the three independent datasets. The integrated zonation identified 9.40% of the study area as high groundwater potential, 89.46% as moderate potential, and only 1.14% as low potential. The incorporation of independent geophysical and hydrogeological evidence significantly reduced uncertainty and enhanced confidence in groundwater potential predictions.

Comparative validation using ROC–AUC performance assessment demonstrated that the integrated model consistently outperformed the individual GIS/RS, VES, and borehole models in predicting groundwater occurrence. The superior predictive capability of the integrated approach confirms that combining surface environmental information with subsurface geophysical measurements and borehole productivity records provides a more accurate representation of basement aquifer systems than reliance on any single dataset. This validates the effectiveness of integrated hydrogeophysical modelling as a reliable framework for groundwater assessment in crystalline basement terrains.

The findings of this study have important implications for groundwater exploration, water supply planning, and sustainable resource management within the Federal Capital Territory and other Basement Complex regions. The integrated groundwater potential model can serve as a practical decision-support tool for optimizing borehole siting, reducing drilling failures, minimizing exploration costs, and improving groundwater development strategies. Future studies should incorporate long-term groundwater level monitoring, aquifer pumping-test analyses, groundwater quality assessment, machine learning algorithms, and higher-resolution geophysical datasets to further enhance groundwater potential prediction and improve the resilience of groundwater resource management under increasing climatic and anthropogenic pressures.

REFERENCES

[1]. Abdulbariu, I., Izge, H. J., Aminu, M. B., Osumanu, J., Ayinla, H. A., Appiah, D., & Ibrahim, I. O. (2024). Geophysical Characterization Of Basement Rock For Groundwater And Mineralization Potential Using Very Low Frequency – Electromagnetic (Vlf-Em) Techniques At Site “G” Around Ibadan Metropolis, Southwestern Basement Complex, Nigeria. *Geological Behavior*, *8*(1), 13–22. https://doi.org/10.26480/gbr.01.2024.13.22

[2]. Abera, B., & Gebre-Egziabher, T. (2024). Remote sensing and GIS supported groundwater potential zone mapping for sustainable groundwater management in Fentale district, Ethiopia. In *Research Square*. https://doi.org/10.21203/rs.3.rs-4184811/v1

[3]. Adegoke, J. A., Ogunseye, T. T., Tsado, G. N., Adefuwa, A. A., & Adeleke, A. A. (2025). Hydrogeophysical Investigation of Groundwater Potential in the Complex Basement of Idu Industrial Area, Federal Capital Territory, Abuja. *Nigerian Journal of Physics*, *34*(4), 107–118. doi:https://doi.org/10.62292/10.62292/njp.v34i4.2025.353

[4]. Adeniji, A., Obiora, D. N., Omonona, O. V., & Ayuba, R. (2013). Geoelectrical evaluation of groundwater potentials of Bwari basement area, Central Nigeria. *International Journal of the Physical Sciences*, *8*(25), 1350–1361. https://doi.org/10.5897/ijps2013.3951

[5]. Agbotui, P. Y., Ewusi, A., Seidu, J., Brookman-Amissah, M., Woode, A., & Aforla, B. (2023). Delineation of preferential flow pathways in a tropical crystalline rock aquifer in Tarkwa, Ghana using

ISSN No:-2456-2165 https://doi.org/10.38124/ijisrt/26jun1770

integrated hydrogeophysical methods. *Hydrology Research*, *54*(5), 722-738.

[6]. Agunleti, Y. S., & Arikawe, E. A. (2014). Groundwater targeting within the basement complex rocks of federal capital territory abuja using remotely sensed and vertical electrical sounding Data. *International Journal of Technology Enhancements and Emerging Research*, *2*(12), 38-47.

[7]. Ajadi, J., Yusuf, M. A., Omolaiye, G. E., Adam, S. B., & Alade, A. D. (2025). Evaluation of groundwater resources using remote sensing and GIS techniques within Kwara State University, Malete, Nigeria. *Discover Geoscience*, *3*(1). https://doi.org/10.1007/s44288-025-00244-0

[8]. Ajayi, O. G., Nwadialor, I., Odumosu, J. O., Adetunji, O. O., & Abdulwasiu, I. O. (2022). Assessment and delineation of groundwater potential zones using integrated geospatial techniques and analytic hierarchy process. *Applied Water Science*, *12*(12). https://doi.org/10.1007/s13201-022-01802-4

[9]. Akoachere, R. A. I., Yaya, O. O., Eyong, A. T., Ayuk, E. O., & Egbe, E. S. (2019). Hydrogeology of Abuja FCT-Nigeria: A GIS Evaluation. *OALib*, *6*(8), 1–35. https://doi.org/10.4236/oalib.1105649

[10]. Alao, J. O., Lawal, H. A., Abdulsalami, M., Abubakar, F., Abduwahab, O. O., Mary, E. T., & Yusuf, M. A. (2024a). Delineation of aquifer storage potential in response to regional groundwater development. *Discover Water*, *4*(1). https://doi.org/10.1007/s43832-024-00084-y

[11]. Alao, J. O., Lawal, H. A., Abubakar, F., & Abdulsalami, M. (2024b). Geophysical and physicochemical assessment of groundwater and the implication on the public health in rural and semi-urban areas of Northern Nigeria. *Discover Environment*, *2*(1). https://doi.org/10.1007/s44274-024-00074-w

[12]. Arulbalaji, P., Padmalal, D., & Sreelash, K. (2019). GIS and AHP Techniques Based Delineation of Groundwater Potential Zones: a case study from Southern Western Ghats, India. *Scientific Reports*, *9*(1), 2082–2082. https://doi.org/10.1038/s41598-019-38567-x

[13]. Awuh, M. E., Japhets, P. O., Officha, M. C., Okolie, A. O., & Enete, I. C. (2019). A Correlation Analysis of the Relationship between Land Use and Land Cover/Land Surface Temperature in Abuja Municipal, FCT, Nigeria. *Journal of Geographic Information System*, *11*(1), 44–55. https://doi.org/10.4236/jgis.2019.111004

[14]. Baghel, S., Tripathi, M. P., Khalkho, D., Al-Ansari, N., Kumar, A., & Elbeltagi, A. (2023). Delineation of suitable sites for groundwater recharge based on groundwater potential with RS, GIS, and AHP approach for Mand catchment of Mahanadi Basin. *Scientific Reports*, *13*(1), 9860–9860. https://doi.org/10.1038/s41598-023-36897-5

[15]. Barman, J., Zuali, F. V., Bindajam, A. A., Mallick, J., & Abdo, H. G. (2024). Detection of groundwater conditioning factors in a hilly environment. *Applied Water Science,*, *14*(4), 88. doi:https://doi.org/10.1007/s13201-024-02139-w

[16]. Bayode, S., Mogaji, K. A., & Egbeyemi, O. (2024). Modeling of geophysical derived parameters for groundwater potential zonation using GIS-based multi-criteria conceptual model. *Applied Water Science*, *14*(2). https://doi.org/10.1007/s13201-023-02056-4

[17]. Bennett, G. (2023). Analysis of methods used to validate remote sensing and GIS-based groundwater potential maps in the last two decades: A review. *Geosystems and Geoenvironment*, *3*(1), 100245–100245. https://doi.org/10.1016/j.geogeo.2023.100245

[18]. Dars, R., Ping, J., Mei, X., & Shah, S. A. (2024). Delineation of groundwater prospective zones using multivariate and spatial analysis techniques in Henan Province North China Plain. *Applied Water Science*, *14*(4). https://doi.org/10.1007/s13201-024-02137-y

[19]. Ebukiba, E. S., & Adamu, S. (2020). Consumers' Choice Of Market Outlets For Fresh Leafy Vegetables Among Rural And Urban Households In Federal Capital Territory, Nigeria. *Russian Journal of Agricultural and Socio-Economic Sciences*, *104*(8), 197–211. https://doi.org/10.18551/rjoas.2020-08.22

[20]. Emmanuel, A., Wasiu, O. O., & Eyankware, M. O. (2024). Delineation Of Groundwater Potential Using Electrical Resistivity Imaging Techniques At Ibule Akure, Southwestern Nigeria. *Malaysian Journal of Geosciences*, *8*(1), 1–9. https://doi.org/10.26480/mjg.01.2024.01.09

[21]. Falebita, D., Olajuyigbe, O., Sunday, A. S., Christopher, O., & Aderoju, A. (2020). Interpretation of geophysical and GIS-based remote sensing data for sustainable groundwater resource management in the basement of north-eastern Osun State, Nigeria. *SN Applied Sciences,*, *2*(9), 1608.

[22]. Farouq, A. U., Mallam, A., & Osagie, A. U. (2025). Hydrogeological Evaluation of Abuja Municipal Area Council (AMAC) Using Vertical Electrical Sounding (VES). *International Journal of Innovative Science and Research Technology (IJISRT)*, 2178–2178. https://doi.org/10.38124/ijisrt/25nov1302

[23]. Gandhi, F. R., Songara, J., Prakash, I., & Altuwaijri, H. A. (2024). Comparative Assessment of Analytical Hierarchy Process (AHP) and Fuzzy Overlay Analysis (FOA) Models in Groundwater Potential Zone Mapping Using Sensitive Analysis: A GIS-RS Integrated Approach. In *Research Square*. https://doi.org/10.21203/rs.3.rs-4368423/v1

[24]. Ibrahim, E. S., Chiroma, J. T., Abubakar, M. A., Ojih, S. A., Waziri, E. S., Daffi, R. E., & Yenne, E. Y. (2024). Spatial modelling of present and future groundwater potentials in Nigeria; towards a sustainable water demand and supply. *Sustainable Water Resources*

Management, *10*(4). https://doi.org/10.1007/s40899-024-01107-1

[25]. Ifediegwu, S. I. (2022). Assessment of groundwater potential zones using GIS and AHP techniques: a case study of the Lafia district, Nasarawa State, Nigeria. . *Applied Water Science*, *12*(1), 10.

[26]. Ideki, O., & Weli, V. E. (2019). Analysis of Rainfall Variability Using Remote Sensing and GIS in North Central Nigeria. *Atmospheric and Climate Sciences*, *9*(2), 191–201. https://doi.org/10.4236/acs.2019.92013

[27]. Jhariya, D. C., Kumar, T., Gobinath, M., Diwan, P., & Kishore, N. (2016). Assessment of groundwater potential zone using remote sensing, GIS and multi criteria decision analysis techniques. *Journal of the Geological Society of India*, *88*(4), 481–492. https://doi.org/10.1007/s12594-016-0511-9

[28]. Jimoh, M. O., Opawale, G. T., Ejepu, J. S., Abdullahi, S., & Agbasi, O. E. (2023). Investigation of Groundwater Potential Using Geological, Hydrogeological and Geophysical Methods in Federal University of Technology, Minna, Bosso Campus, North Central, Nigeria. *HydroResearch*, *6*, 255–268. https://doi.org/10.1016/j.hydres.2023.09.002

[29]. Jothibasu, A., & Anbazhagan, S. (2016). Modeling groundwater probability index in Ponnaiyar River basin of South India using analytic hierarchy process. *Modeling Earth Systems and Environment*, *2*(3). https://doi.org/10.1007/s40808-016-0174-y

[30]. Karandish, F. L. (2025). Global groundwater sustainability: A critical review of strategies and future pathways. *Journal of Hydrology,*, *657*, 133060–133060. doi:https://doi.org/10.1016/j.jhydrol.2025.133060

[31]. Kareem, H. H. (2024). Groundwater potential zone mapping of Llandrindod Wells, Wales, UK using GIS, remote sensing, and analytic hierarchy process. *Journal of Water and Climate Change,*, *15*(11), 5606-5625.

[32]. Karim, H. A., & Al-Manmi, D. A. (2019). Integrating GIS-based and geophysical techniques for groundwater potential assessment in Halabja Said Sadiq sub-basin, Kurdistan, NE Iraq. *Tikrit Journal of Pure Science,*, *24*(6), 81-92.

[33]. Mangs, A. D., Ejepu, J. S., Nkemkah, C. C., Yusuf, S. N., Sallau, A., Yakubu, J. A., Ibrahim, Y., & Wakili, W. M. (2023). Groundwater Potential Mapping in Lapan Gwari Community Using Integrated Remote Sensing and Electrical Resistivity Soundings. *International Journal of Geosciences*, *14*(8), 719–732. https://doi.org/10.4236/ijg.2023.148039

[34]. Musekiwa, C., Penn-Clarke, C. R., Nhleko, L. O., Charles, A., Phikiso, Z., & Dhansay, T. (2025). Assessing groundwater potential using GIS-MCDM and remote sensing techniques: A case study of Franschhoek, South Africa. *Water SA*, *51*. https://doi.org/10.17159/wsa/2025.v51.i4.4119

[35]. Naghibi, S. A., Pourghasemi, H. R., & Dixon, B. (2016). GIS-based groundwater potential mapping using boosted regression tree, classification and regression tree, and random forest machine learning models in Iran. *Environmental monitoring and assessment,*, *188*(1), 44.

[36]. Nainggolan, L., Ni, C. F., Darmawan, Y., Lo, W. C., Lee, I. H., Lin, C. P., & Hiep, N. H. (2024). Cost-effective groundwater potential mapping by integrating multiple remote sensing data and the index–overlay method. *Remote Sensing,*, *16*(3), 502.

[37]. Naiyeju, J. O., Oladunjoye, M. A., & Adeniran, M. A. (2021). Aquifer evaluation in parts of north-central Nigeria from geo-electrical derived parameters. *Applied Water Science*, *11*(11). https://doi.org/10.1007/s13201-021-01520-3

[38]. Noma, T. A. J., Bakr, A. F., & Elsayad, Z. M. (2022). Methodological Approach To Incorporating Hausa Traditional Architecture In Urban Development: The Case Of Abuja, Nigeria. *WIT Transactions on Ecology and the Environment*, *1*, 465–475. https://doi.org/10.2495/sc220381

[39]. Obiadi, B. N., Ezezue, A. M., & Uduak, P. U. (2019). Abuja: Nigeria's Spatial Economic Turmoil and Urban Development Disarray. *Current Urban Studies*, *7*(3), 371–398. https://doi.org/10.4236/cus.2019.73019

[40]. Ogundana, A. K., & Falae, P. O. (2024). Groundwater potential modelling and aquifer zonation of a typical basement complex terrain: a case study. *Environment Development and Sustainability*, *27*(12), 31081–31103. https://doi.org/10.1007/s10668-024-04940-8

[41]. Olorunfemi, M. O., Oni, A. G., Bamidele, O. E., Fadare, T. K., & Aniko, O. O. (2020). Combined geophysical investigations of the characteristics of a regional fault zone for groundwater development in a basement complex terrain of South-west Nigeria. *SN Applied Sciences*, *2*(6). https://doi.org/10.1007/s42452-020-2363-6

[42]. Omeje, M., Ejike, E. J., & Ugwuoke, P. E. (2015a). *Geophysical Analysis of Basement Terrain Groundwater Using Vertical Electrical Sounding: A Case Study of Parts of Abuja North Central Nigeria*.

[43]. Omeje, M., Ejike, J. E., & Ugwuoke, P. E. (2015b). *Geophysical Analysis of BasementTerrain Groundwater Using VerticalElectrical Sounding: A Case Study ofParts of Abuja North Central Nigeria*. http://eprints.covenantuniversity.edu.ng/10671/

[44]. Osumeje, J. O., Eshimiakhe, D., Oniku, A. S., & Lawal, K. M. (2023). Application of Remote Sensing and Geophysical Methods for Delineating Groundwater Potential at North Western Nigeria. In *Research Square*. https://doi.org/10.21203/rs.3.rs-3758890/v1

[45]. Pande, C. B., Moharir, K. N., Panneerselvam, B., Singh, S. K., Elbeltagi, A., Pham, Q. B., Varade, A. M., & Rajesh, J. (2021). Delineation of groundwater potential zones for sustainable development and planning using analytical hierarchy process (AHP),

and MIF techniques. *Applied Water Science*, *11*(12). https://doi.org/10.1007/s13201-021-01522-1

[46]. Pandian, R., Sıdesh, U., K, P. B., & R, L. N. (2023). Identification of groundwater potential for urban development using multi-criteria decision-making method of analytical hierarchy process. *International Journal of Engineering and Geosciences*, *8*(3), 318–328. https://doi.org/10.26833/ijeg.1190998

[47]. Rajesh, J., Pande, C. B., Kadam, S. A., Gorantiwar, S. D., & Shinde, M. G. (2021). Exploration of groundwater potential zones using analytical hierarchical process (AHP) approach in the Godavari river basin of Maharashtra in India. *Applied Water Science*, *11*(12). https://doi.org/10.1007/s13201-021-01518-x

[48]. Roy, D., Barman, S., Mandal, G., Mitra, R., Sarkar, A., Hossain, G. M. A., Roy, P., Almohamad, H., Abdo, H. G., & Mandal, D. K. (2024). Extracting of prospective groundwater potential zones using remote sensing data, GIS, and multi-criteria decision-making approach in the Sub-Himalayan Dooars region of West Bengal, India. *Applied Water Science*, *14*(4). https://doi.org/10.1007/s13201-024-02124-3

[49]. Saaty T. L. (1980). The analytic hierarchy process. Agric Econ Rev. 1980;70(804):10-21236.

[50]. Salem, Z. E., Temamy, A. M. A., Abu-Alam, T., Mesallam, M. A., & Fahil, A. S. (2025). Integration of geospatial technology and AHP model for assessing groundwater potentiality in Arid Regions: a case study in Wadi Araba Basin, Western Coast of Gulf of Suez, Egypt. *Frontiers in Marine Science*, *12*. https://doi.org/10.3389/fmars.2025.1670000

[51]. Sanusi, S. O., Madaki, M. J., David, H. S., & Adole, S. O. (2021). Land Tenure Systems and Agricultural Productivity in Nigeria: a Case of Rice Production. In *Research Square*. https://doi.org/10.21203/rs.3.rs-1008949/v1

[52]. Shekar, P. R., & Mathew, A. (2023). Delineation of groundwater potential zones and identification of artificial recharge sites in the Kinnerasani Watershed, India, using remote sensing-GIS, AHP, and Fuzzy-AHP techniques. *AQUA - Water Infrastructure Ecosystems and Society*, *72*(8), 1474–1498. https://doi.org/10.2166/aqua.2023.052

[53]. Shinde, S. P., Barai, V. N., Gavit, B. K., Kadam, S. A., Atre, A. A., Pande, C. B., Pal, S. C., Radwan, N., Tolche, A. D., & Elkhrachy, I. (2024). Assessment of groundwater potential zone mapping for semi-arid environment areas using AHP and MIF techniques. *Environmental Sciences Europe*, *36*(1). https://doi.org/10.1186/s12302-024-00906-9

[54]. Sunkari, E. D., Kore, B. M., & Abioui, M. (2021). Hydrogeophysical appraisal of groundwater potential in the fractured basement aquifer of the federal capital territory, Abuja, Nigeria. *Results in Geophysical Sciences*, *5*, 100012–100012. https://doi.org/10.1016/j.ringps.2021.100012

[55]. Tabassum A, Sajjad A, Sajid GH, Ahmad MIM, Khan AH. (2025). Assessing recharge zones for groundwater potential in Dera Ismail Khan (Pakistan): a GIS-based analytical hierarchy process approach. Water. 2025;17(11):1586.

[56]. Taher, M., Mourabit, T., Etebaai, I., Dekkaki, H. C., Amarjouf, N., Amine, A., Bourjila, A., Errahmouni, A., & Azzouzi, S. (2023). Identification of Groundwater Potential Zones (GWPZ) Using Geospatial Techniques and AHP Method: a Case Study of the Boudinar Basin, Rif Belt (Morocco). *Geomatics and Environmental Engineering*, *17*(3), 83–105. https://doi.org/10.7494/geom.2023.17.3.83

[57]. Tehrany, M. S., Pradhan, B., M. S., & Ahmad, N. (2015). Flood susceptibility assessment using GIS-based support vector machine model with different kernel types. *Catena*, *125*, 91-101.

[58]. Velis, M., Conti, K. I., & Biermann, F. (2017). Groundwater and human development: synergies and trade-offs within the context of the sustainable development goals. *Sustainability Science*, *12*(6), 1007–1017. doi:https://doi.org/10.1007/s11625-017-0490-9.

[59]. Zewdie, M. M., Kasie, L. A., & Bogale, S. (2024). Groundwater potential zones delineation using GIS and AHP techniques in upper parts of Chemoga watershed, Ethiopia. *Applied Water Science*, *14*(4). https://doi.org/10.1007/s13201-024-02119-0.